WCTE 2016
World Conference on Timber Engineering
August 22-25, 2016 | Vienna, Austria

HOLES IN GLULAM – ORIENTATION AND DESIGN OF INTERNAL REINFORCEMENTS

Cristóbal Tapia[1], Simon Aicher[2]

ABSTRACT: The usage of holes in glulam and LVL beams is a common practice in timber constructions and requires in many cases the application of reinforcement. At present, Eurocode 5 does not contain design rules for holes, nor for their reinforcement, which are, however, regulated in the German National Annex to EC5. Although it has been proven that internal rod-like reinforcements improve the shear force capacity of a beam with holes, several problems still remain, particularly the inability to successfully reduce peak stresses at the periphery of the hole, especially shear stresses. Inclined internal steel rod reinforcements were studied and compared with vertically oriented rods, which is currently the only regulated application. The analysis revealed a reduction of both perpendicular to grain tensile stresses and shear stresses, which for the case of vertical rods are not reduced at all. A first attempt at the design of such inclined reinforcements was made by deriving an equation based on the results from FEM simulations. The design approach was then applied to an example case. Experimental verification of the theoretical observations is still necessary and ongoing, though a very promising approach for an improved internal reinforcement and its respective design can already be observed.

KEYWORDS: glulam, holes, internal reinforcements, design equations, Eurocode 5

1 INTRODUCTION

The use of large holes in beams made of glulam (GLT) or laminated veneer lumber (LVL) is often necessary in constructions, as they are required for the passing-through of plumbing, electrical and other service relevant infrastructure systems. These apertures represent a significantly weak region in the beam, leading to noticeable decreases in maximum loading capacities.

The failure mechanism is well known and is manifested by the propagation of cracks in the direction of the grain and beam length axis, starting from two zones with high tensile stresses perpendicular to the grain located diagonally opposite on the periphery of the hole, as shown in Figure 1.

The European Timber Design Code, EN 1995-1-1 [1] also known as EC5, contains no provisions for either unreinforced or reinforced holes. The current version of the German National Annex to EC5 [2] regulates external plate-type hole reinforcements, as well as the usage of internal, rod-like reinforcements to improve the mechanical response of the glulam/LVL in the region surrounding a given aperture. The internal reinforcements are normally preferred to external, plate-like ones, since, from a feasibility standpoint, they are easily applied with rather low cost, and from an architectural/aesthetics standpoint, they are invisible, as they are embedded in the glulam/LVL beam. The positive effect of internal rod reinforcements on ultimate load of a beam with a hole has been proven both experimentally and by means of computer simulations in [3]. In this study some downsides to internal rod reinforcements were seen, the most important of which being the inability of this kind of reinforcement to reduce the shear stresses at the critical regions where cracks are expected to occur [3]. Further, such shear stresses were found to be of great relevance for the long-term crack growth in the vicinity of the hole. The use of inclined rod-like internal reinforcements was experimentally studied in [4] for rectangular holes, where a clear improvement in load bearing capacity was observed. This was explained as an increased stiffness of the beam on the region of the hole, which leads to a reduction in the shear stresses at the periphery of the hole. Further results of this promising approach could not be found in literature.

2 DESIGN OF HOLE REINFORCEMENT ACCORDING TO GERMAN NATIONAL ANNEX TO EN 1995-1-1

The present design of hole reinforcements according to DIN EN 1995-1-1/NA [2] is based, analogously to the verification of unreinforced holes, on a fictive tensile force, $F_{t,90}$, composed of two additive parts: one accounting for the shear force part, which cannot be transferred in the hole area, and a second part related to the moment present in the cross-section:

[1] Cristóbal Tapia Camú, MPA University of Stuttgart, Germany, cristobal.tapia-camu@mpa.uni-stuttgart.de
[2] Simon Aicher, MPA University of Stuttgart, Germany, simon.aicher@mpa.uni-stuttgart.de

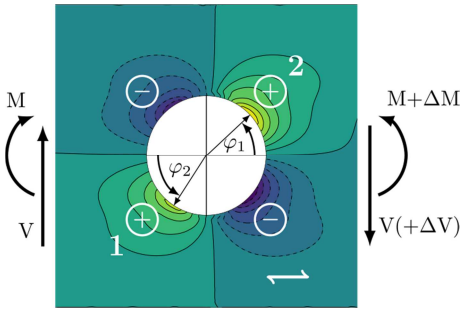

Figure 1: *Distribution of stresses perpendicular to the grain in the vicinity of a hole in a glulam beam, in a zone subjected to shear force and moment*

$$F_{t,90} = F_{t,V} + F_{t,M} \tag{1}$$

$$F_{t,V} = \frac{V \cdot h_d}{4 \cdot h}\left(3 - \frac{h_d^2}{h^2}\right) \tag{2}$$

$$F_{t,M} = 0.008 \cdot \frac{M}{h_r} \quad . \tag{3}$$

The shear force part, $F_{t,V}$, conforms sensibly to half of the integral of the parabolically distributed shear stresses along the full hole depth (rectangular hole) or 0.7 times of the hole depth for the case of the round holes regarded here. The moment related part, $F_{t,M}$, is in contrast rather diffuse and needs amendment, as discussed previously in [5]. The dimensional notation of reinforced holes according to [2] is shown in Figure 2.

3 VERIFICATION OF REINFORCEMENTS BY TEST RESULTS

In a brief summary of previous investigations reported in [3] the following issues are noteworthy. Although the study was limited to glulam beams with a depth of 450 mm (beam width = 120 mm) and a hole diameter to beam depth ratio, h_d/h, of 0.4, exceeding the currently allowed limits for screwed reinforcements [2], the test indicates an improvement in the load bearing capacity due to internal reinforcements with vertical rods. Test series comparing beams with unreinforced and reinforced holes for which self-tapping screws and glued-in rods (applied perpendicular to beam axis) were used, showed that the reinforced beams did not fully reach the load capacities predicted by the approach currently used in [2]. It was shown that on average the ultimate shear force reached was 40% lower as compared to the ultimate share force of the full cross section.

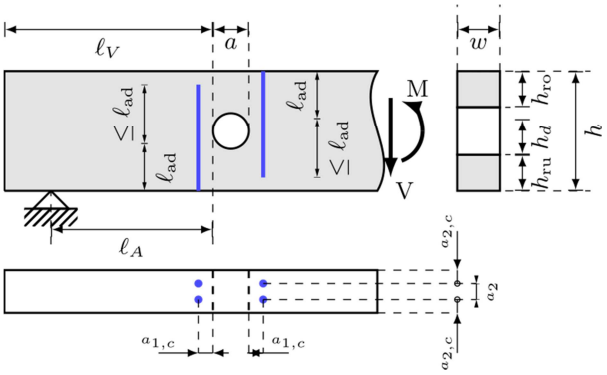

Figure 2: *Dimensional notations of reinforced round holes according to* ***[2]***

4 STRESS DISTRIBUTIONS AT HOLES WITH INCLINED ROD REINFORCEMENTS

4.1 FINITE ELEMENT MODEL

Using the Finite Element Method (FEM) a parametric model of a beam with a hole and inclined internal reinforcements was created, for which the software Abaqus 2016 was employed. The elements chosen for the glulam were linear 3-dimensional hexagonal elements with reduced integration (C3D8R). The rods were also modeled as 3-dimensional continua using the same elements as used for the glulam. The interaction on the interface of both materials (glulam and reinforcements) was described by means of so-called "*Tie constraints*", applied to the respective surface pairs in contact, except for the end face of the rods, as the force should only be transferred by the side areas of the rods (modeled as cylinders). The employed material properties of the glulam (built up homogeneously, exclusively from one lamination strength class) corresponded to strength class GL32h according to EN 14080 [6] and are summarized in Table 1, along with the properties used for the steel rods.

The dimensions of the glulam beam modeled in the parametric study are shown in Figure 3a.The hole was placed centrally between the support and the point of load application, in the constant shear area, with a shear force to moment ratio V/M = 1.03. Although the FEM model was designed parametrically, for this study only a ratio $h_d/h = 0.3$ was used. The diameter, length and inclination of the rod are free parameters. Symmetry was applied on two planes, the first one at mid-span, on the plane containing the cross-section (ZY-plane) and the second one located at mid-width (z=0), on the vertical plane cutting the beam in the longitudinal direction (XY-plane). The rotation points of the reinforcements with different inclinations β vs. the vertical axis (Figure 3b) were defined to be at the intersection of a vertical line located at a horizontal distance from the hole edge of 2.5 times the diameter of the rod, d_r, and a horizontal line starting at the periphery of the hole, at an angle of φ = 45° (+180°, accordingly) with respect to the horizontal direction (see Figure 3). The reasoning behind the choice of the specific rotation points, is that the maximum stresses perpendicular to the grain (σ_y) are expected to occur under an angle $\varphi \approx 45°$ (+180°), which also defines the most probable/empirically verified crack surface. The stresses observed on this surface are used for comparison of the effect of the different inclinations β. With regard to the above, it is therefore desirable to maintain the distance between the hole periphery and rod axis constant, by rotating the rod around the specified rotation point.

Table 1: *Material properties used for the glulam and the steel rods in the FEM model*

Material	$E_{(x)}$ N/mm^2	E_y N/mm^2	E_z N/mm^2	$\upsilon_{(xy)}$ N/mm^2	υ_{xz} N/mm^2	υ_{yz} N/mm^2	G_{xy} N/mm^2	G_{xz} N/mm^2	G_{yz} N/mm^2
GL32h	13000	430	430	0.02	0.02	0.2	810	810	81
Steel	210000	–	–	0.3	–	–	–	–	–

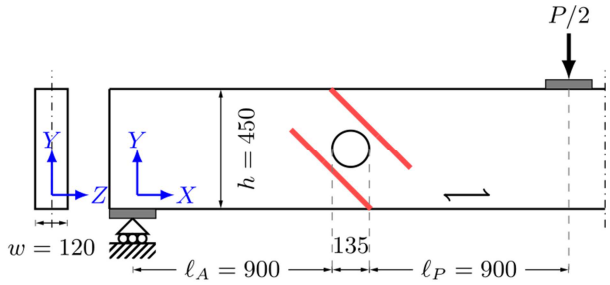

(a)

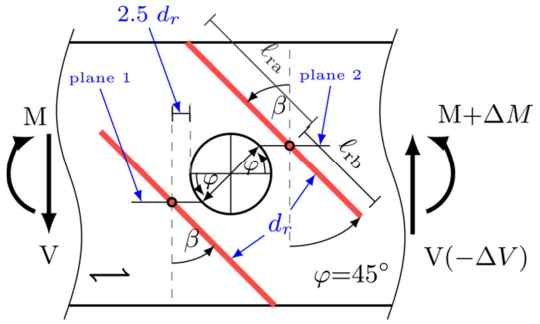

(b)

Figure 3: *(a) Dimensions of the glulam beam and hole used for the FEM simulations; (b) positioning and orientation of internal reinforcements, and notations of the different dimensions used.*

The mesh size on the perimeter of the hole was chosen to be around 2 mm and increases slightly (to 3 mm) on the region surrounding the rod. Along the direction of the beam width, the elements had a length of 5 mm. Figure 4a depicts the meshing at the vicinity of the hole for reinforcements with inclination angle $\beta = 45°$.

The damaged situation, in which a crack has spread horizontally along planes 1 and 2 accordingly (see Figure 3b), starting from the periphery of the hole, was modeled using the Extended Finite Element Method (XFEM). Accordingly, an unmeshed surface was placed in the position of the expected crack location up to the rod axis, which automatically cuts the enriched elements it intersects. Note: no crack growth was considered in this specific analysis, but only the effect of one fully developed crack on the stresses and rod forces was regarded. This means that no considerations regarding fracture mechanics were taken.

4.2 STRESSES IN THE UNDAMAGED GLULAM

The effect of different angles of the rods was analyzed in a parametric study. Stresses perpendicular to the grain direction (σ_y) along with shear stresses (τ_{xy}) were evaluated on the mentioned planes 1 and 2, where highly elevated stresses at the hole vicinity occur. In the following, exemplary results for a rod diameter of $d_r = 18$ mm, lengths $\ell_{rb} = 200$ mm and cross-sectional width $w = 120$ mm are discussed. Figure 5a and Figure 5b show the tensile stresses perpendicular to the grain in plane 2 of the glulam with reinforcements inclined by angles $\beta = 0°$, i.e. vertically oriented bars, and $\beta = 45°$, respectively, compared to the case where no reinforcement is used. A marked reduction of the tensile stresses perpendicular to the grain can be observed along the length and width directions of plane 2 for the situation where the rod is rotated by 45°, shown in Figure 5b, as compared to Figure 5a, depicting the stress situation for the vertically placed internal reinforcements. For the case of the vertical rods, stresses σ_y directly at the periphery of the hole (Figure 5a) are reduced only slightly between 5% at ± w/2 and 14% at mid-width with respect to the unreinforced case. In contrast, the stresses σ_y at the same locations are reduced by 28% and 40%, respectively, in case of the inclined rods ($\beta = 45°$). Furthermore the σ_y stress reduction is far more uniform as for the case with vertical rods.

Regarding the effect on shear stresses, as expected, the inclined rods resulted in throughout plane 2 a significant

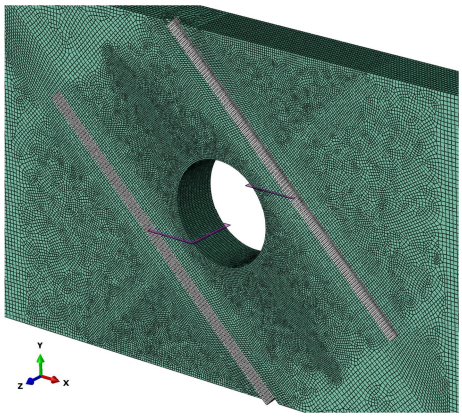

(a)

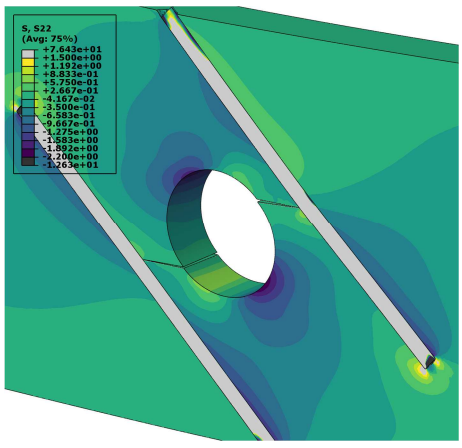

(b)

Figure 4: *(a) Discretization of the FEM model in the vicinity of the hole and location of internal reinforcements and crack planes; (b) Stresses perpendicular to grain obtained with the FEM model for a rod diameter of d_r=18 mm and an inclination $\beta = 45°$*

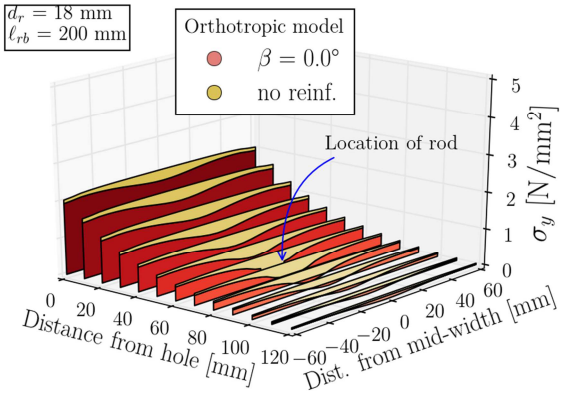

(a)

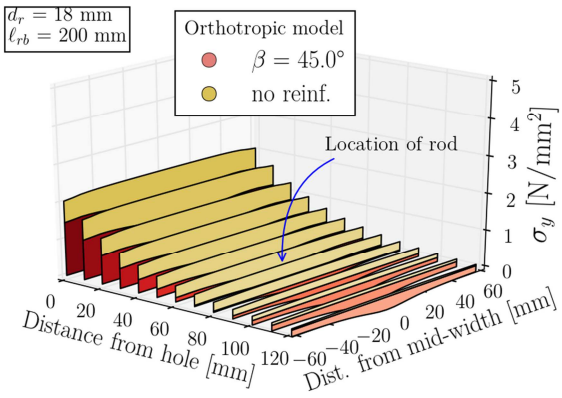

(b)

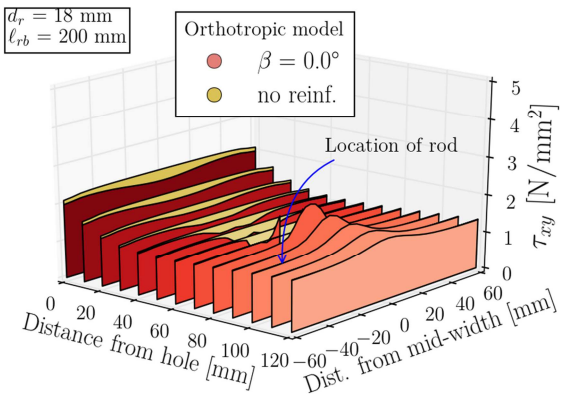

(c)

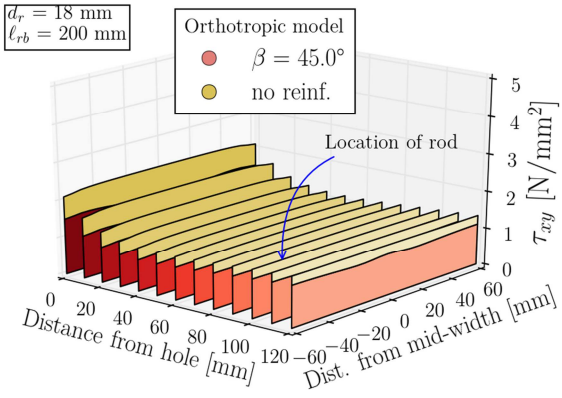

(d)

Figure 5: *Comparison of stress distributions on plane 2 (see Figure 3) between the unreinforced situation and glulam reinforced with internal rods at inclinations of β = 0° and β = 45°. Figs. (a) and (b) show stresses perpendicular to grain and Figs. (c) and (d) represent the shear stresses.*

reduction of 30% to 40% vs. the unreinforced state as shown in Figure 5d. Conversely, the vertical rods are almost ineffective (reductions of 5% to 14% between hole periphery and rod), and even lead to shear stress increase, when regarding locations beyond the distance between hole and rod (Figure 5c).

Observing these results, it could be concluded that the internal reinforcement has effectively taken up about 34% of the shear force responsible for the stresses on the analyzed region. This percentage was calculated as the mean of the previously given values, obtained at the borders and mid-width of the glulam. For the region located on plane 1, the reduction of the shear force in the glulam is even higher, reaching approximately 47%. At this point it has to be noted that these values are not calculated on the basis of the maximum stresses at the periphery of the hole, but rather from the values obtained at φ = 45°. When considering the maximum stresses perpendicular to the grain (not necessarily lying at the position φ = 45°) it becomes evident that for the upper right region of the hole this value still holds, but for the opposite region (lower left sector of the hole) the shear force is reduced by about 35%, almost the same as what is obtained on plane 2, which makes both sides consistent with each other. The difference is due to the fact that for the case of plane 2 the position of the maximum stresses is very close to φ = 45°, whereas for plane 1 the location of maximum stresses lays under an angle clearly above 45°, which is what normally occurs around holes under these loading conditions [7].

4.3 STRESSES IN THE DAMAGED GLULAM

The redistribution of the analyzed stresses, σ_y and τ_{xy}, in the damaged situation, induced by the horizontal crack in planes 1 and 2 (see Figure 3b), is depicted in Figure 6a and Figure 6b. Each figure compares the results obtained for the glulam with rod inclinations of β = 0° and β = 45°. It can be observed that the stresses perpendicular to the grain in Figure 6a are successfully reduced by the presence of the vertical rod, but still show a small peak at the crack tip, while for the inclined reinforcement the stresses are further reduced to a significant degree. In case of the shear stresses (Figure 6b) it can be seen that they suffered absolutely no change in the region preceding the reinforcement, having practically the same values as observed in the situation without crack in Figure 5c. It is interesting to see that in the case of the inclined rod, the shear stresses maintain a level only slightly higher as in the undamaged situation, which shows that the length of the crack has apparently no effect on the shear stresses.

4.4 FORCES ALONG REINFORCEMENTS

It has been shown that an effective reduction of the stresses σ_y and τ_{xy} is achieved if the internal reinforcement is rotated by 45°. In the following, the axial forces in the reinforcements, for the cases previously illustrated, will be presented and discussed, which will later help in the derivation of a design rule for the rod reinforcements.

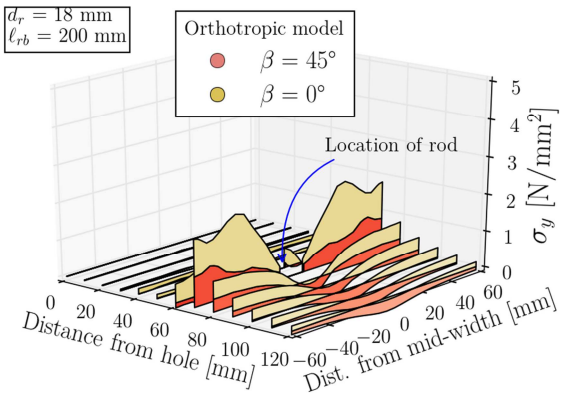

(a)

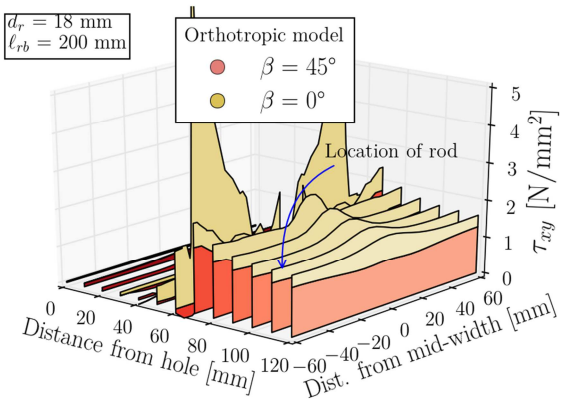

(b)

Figure 6: *Comparison of stress distributions in plane 2 (see Figure 3), with a fully developed crack from the hole periphery to the center of the rod, with rods inclined by $\beta = 0°$ and $\beta = 45°$; (a) shows the stresses perpendicular to grain and (b) depicts the shear stresses.*

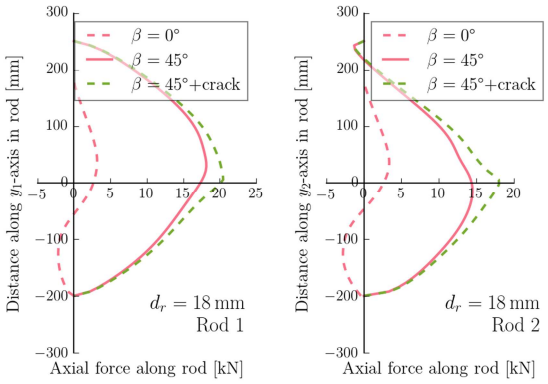

(a) *(b)*

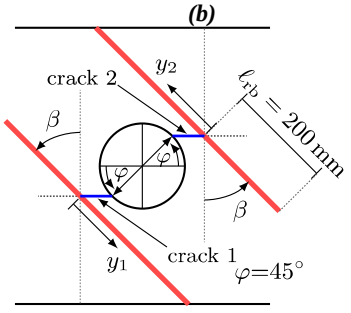

(c)

Figure 7: *Axial forces along the rod reinforcements under inclinations β of 45°. Fig. (a) and (b) show the results for the reinforcement No. 1 and 2, respectively (the left and right reinforcement in (c)).*

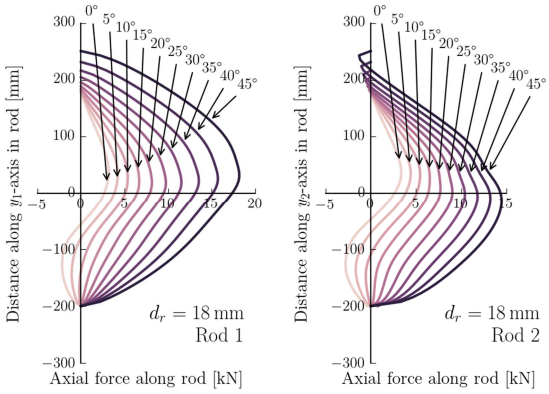

(a) *(b)*

Figure 8: *Axial forces along the rod reinforcements for inclinations β between 0° and 45° in steps of 5°, for a rod of diameter d_r = 18 mm.*

Figures 7a and 7b show the axial forces for the left and right rods in Figure 8c for inclination angles $\beta = 0°$ and $\beta = 45°$. It can be clearly noticed that the axial forces of the inclined reinforcements are significantly higher than in the case of the vertical rods. The maximum forces of the inclined rods are about five and four times (left and right rod, respectively) higher as compared to maximum values of the vertically placed rods. For rod 1, it can be observed that the maximum value of the rod axial force does not lay as close to $y_1 = 0$ as in the case of the rod 2, which is due to the mentioned fact, that the maximum vertical tensile stresses in the stress region 1 (see Figure 1) are located an angle φ larger than 45°. Apart from the highly increased tensile force level in the inclined rods, the second most important fact to state is related to the force distribution along the rods. In the case of the inclined rods, the force is throughout a tensile one, which increases rather parabolically from the rod ends to the maximum value occurring very roughly at $y_{1,2} \approx 0$. This force evolution is very different from the force distribution observed in vertical rods, where a sign change from tensile to compressive force always occurs. Note: The vertical rods exhibit a tensile force throughout the total tensile perpendicular to grain stress regions 1 and 2 but change to compression in the above (rod 1) and below (rod 2) located compression perpendicular to grain region (compare Figure 1).

The location of the maximum value of the axial force should indicate, more or less, the vertical position at which the respective crack will initiate and later propagate. In the presented analysis, however, the cracks at both sides of the hole are placed at $\varphi = 45°$ (planes 1 and 2) for the reasons mentioned in Section 4.1. Figures 7a and 7b also show the forces for the damaged case with $\beta = 45°$, where a moderate increase, with peaks on the crack locations, can be observed.

The evolution of the distribution of axial forces along the rods with increasing inclination angle β can be seen in Figures 8a and 8b. It is interesting to notice that for inclinations greater than 10°, no compressive forces are observed in the reinforcement any longer. This effect is due to the fact that with increasing angles the rod no longer crosses the zone with compressive stresses perpendicular to the grain as is shown in Figure 1. Another

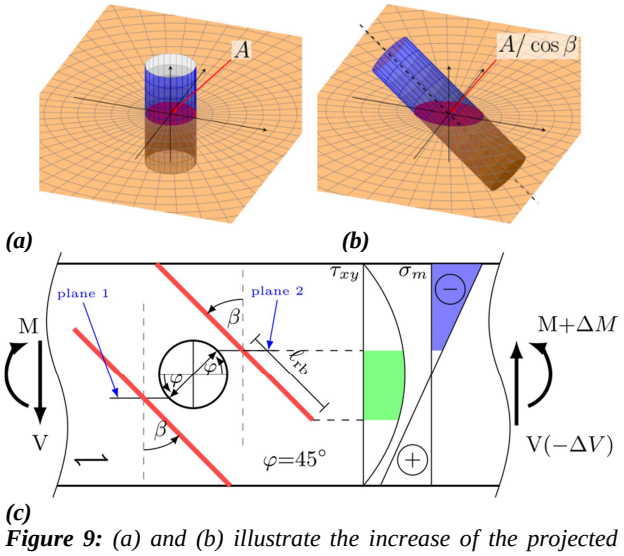

Figure 9: *(a) and (b) illustrate the increase of the projected area of the rod into the crack plane; (c) Design concept for the inclined internal reinforcements*

aspect worth mentioning is the clear effect of the bending stresses (tensile and compressive) that can be observed, when comparing the rods 1 and 2. While the axial forces in the rod 1 for $y_1 > 0$ get noticeably larger with each angle increment, the contrary seems to happen in rod 2, where the axial forces are being restrained, and pulled to the compression zone at the end of the rod.

5 DESIGN MODEL AND DETAILING FOR INCLINED ROD REINFORCEMENTS

A design equation that enables a good assessment of the axial force in the rods should take into account the behavior observed in the presented FEM models. First, it has to be noted that the axial force to be taken into account is the one obtained in the damaged situation (see Figures 7a and 7b). This is due to the fact that, although the maximum stresses at the periphery of the hole are greatly reduced, the possibility for the cracks to initiate is still present, and the rods should be able to resist in this state. Nevertheless, the crack propagation should stop at the location of the internal reinforcement. The other aspect is the angle of inclination, which has at least two effects on the resulting axial force of the rod. One effect is the fact that, looking at the possible crack surface, if the rod is inclined, then the surface of the reinforcements on that plane increases, which should influence the amount of vertical force that is taken by the rod (see Figures 9a and 9b). The other effect is the amount of shear force that the reinforcement takes from the cross-section, before it gets to the critical zone in the vicinity of the hole. The closer the inclination angle β comes to 45°, the more shear force the rod is able to take from the cross section, which at the end reduces the stresses at the periphery of the hole, as previously shown.

$$F_r = \left[\left(F_{r,V} \cdot c_1 + F_{r,M} \cdot c_2 \right) \cdot \sin\beta \cdot \sqrt{\frac{d_r}{w}} + F_{t,90} \cdot c_3 \cdot \frac{d_r}{\sqrt{w}} \right] \cdot \frac{1}{\cos\beta} \tag{4}$$

Based on these observations the below given equation was derived and calibrated with preliminary FEM results:

- $F_{r,V}$: is the integral of the shear force between the end of the rod and the crack plane, as described in Figure 9c (green area),

$$F_{r,V} = \int_{y_0}^{y_1} \frac{V}{2I} \cdot \left(\frac{h^2}{4} - y^2 \right) dy \tag{5}$$

- $F_{r,M}$: is the integral of the bending stresses, as shown in Figure 9c (blue area),

$$F_{r,M} = \int_{y_1}^{y_2} -\frac{M \cdot y}{I} dy \tag{6}$$

- c_1, c_2, c_3: are constants, which are calibrated with FEM results, and have the following values: c_1 = 0.63; c_2 = 0.008; c_3 = 0.36
- d_r: is the diameter of the rod, and
- w: is the width of the cross-section of the beam.

In a further explanation, equation (4) can be divided into three parts. The first part is the term $F_{r,V}$ and accounts for the amount of shear force that goes into the rod in the region not influenced by the hole, which, for simplicity, can be assumed to be the extension of the rod below the crack plane (see Figure 9c). The second part is the one related to the term $F_{r,M}$, which tries to account for the difference in the axial force observed at both sides (left and right), caused by the bending stresses above the crack plane. These stresses pull or compress the rods in the positive and negative bending zones accordingly, and is marked as the blue area in Figure 9c. The third term corresponds to the amount of vertical force that the internal reinforcement takes up at the crack plane, and is here related to the vertical force $F_{t,90}$. The factor $1/\cos\beta$ results from the increase of the projected area of the rod on the crack surface, as shown in Figure 9a and Figure 9b. This increase is also taken into account in the other terms, since the inclination of the rod increases the total volume of reinforcement, which couses the force taken up by the rod to also increase. Finally, the terms $\sqrt{d_r/w}$ and $d_r/\sqrt{w}$ are multiplied accordingly, as presented in equation (4), to properly scale for different cross-sections and rod diameters.

Figures 9a and 9b show the axial forces obtained with the FEM model and with Eq. (4) for diameters d_r = 18 mm and 12 mm and cross-section widths w = 100 mm and 120 mm, for the left and right rein-

forcements. A good agreement between the proposed equation and the axial forces obtained from the simulations can be observed for the range of inclination angles defined by $0° \leq \beta \leq 45°$.

5.1 DESIGN EXAMPLE

In this section, two configurations of a glulam beam with a round hole, reinforced internally by self-tapping screws are regarded. The two configurations differ by the inclination of the rods: Example A considers vertically placed reinforcements, as considered today exclusively in [2], and Example B considers an inclination of the rods by 45°. Both examples are shown in Figure 11. A beam of dimensions $\ell \times h \times w$ = 3500 mm ×450 mm × 120 mm and a span of 3150 mm is loaded at mid-span, and a round hole with diameter of 135 mm is placed at a distance ℓ_A =720 mm, as shown in Figure 11. The properties of the glulam are those of the strength class GL32h, according to EN 14080 [6]. Figure 2a is used to refer to the different dimensions. The distance of the vertical rods from the hole periphery is chosen as 2.5 d_r, specified as the minimum in [2]. In order to give a fair comparison between the vertical and the inclined rod arrangements the effective anchorage length ℓ_{ad} specified in [2] as

$$\ell_{ad} = h_{ru,ro} + 0.15 \cdot h_d = 157.5 + 0.15 \cdot 135 \approx 180\ mm \quad (7)$$

was also chosen for ℓ_{rb}. Note: An inherent advantage of inclined rods consists of the fact that the effective anchorage length can by chosen considerably longer as compared to the vertical rod, where ℓ_{ad} is limited by equation (7).

The screw diameter was chosen as 12 mm, delivering a characteristic pull-out capacity of ($\rho_k = 430\ kg/m^3$)

$$R_{ax,k} = 80 \cdot 10^{-6} \cdot \rho_k^2 \cdot \ell_{ad} \cdot d_r = 14.8 \cdot 180 \cdot 12 = 32.0\ kN \quad (8)$$

In the example, the applied load of 252 kN is chosen such that the characteristic shear capacity of the beam without hole

$$V_k = \frac{2}{3} \cdot 3.5 \cdot 450 \cdot 120 = 126\ kN \quad (9)$$

is reached (considering the hole, the shear capacity would be 88.2 kN).

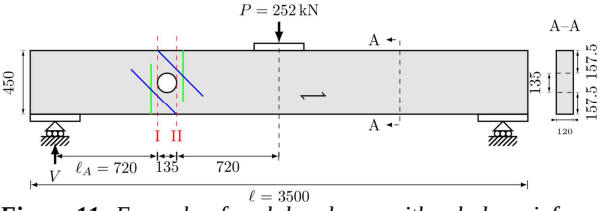

Figure 11: *Example of a glulam beam with a hole, reinforced with inclined rods.*

5.1.1 SECTION FORCES AT BOTH SIDES OF THE HOLE

The section forces at both sides of the hole are:

$$V_I = 126\ kN\ ;\ V_{II} = 126\ kN \quad (10)$$

$$M_I = 90.7\ kNm\ ;\ M_{II} = 107.7\ kNm \quad (11)$$

5.1.2 DETERMINATION OF THE VERTICAL FORCE

Applying Equations (1) to (3), the vertical force $F_{t,90}$ is calculated at sections I and II:

$$F_{t,90,I} = 24.0\ kN\ ;\ F_{t,90,II} = 24.9\ kN \quad (12)$$

5.1.3 DESIGN OF THE RODS

Vertical reinforcements:

For the vertical reinforcements the utilization factor of the reinforcement is given by (evaluated for the rod 2, section II)

$$\frac{F_{t,90}}{R_{ax}} = \frac{24.9}{32.0} = 0.78 < 1 \quad (13)$$

which means that the chosen screw is apt for this case.

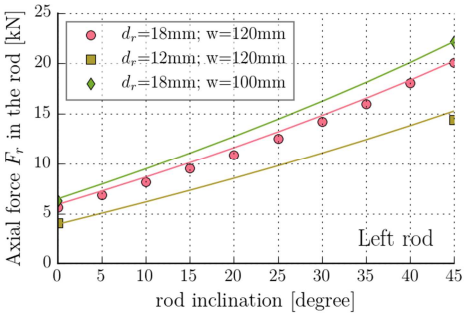

(a)

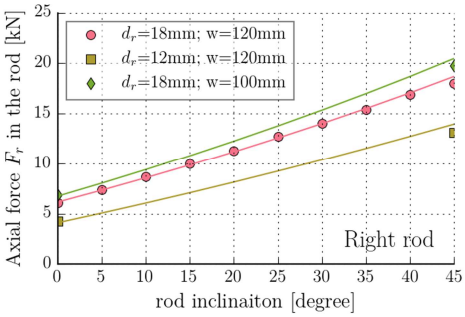

(b)

Figure 10: *Maximum axial force in the rod reinforcement obtained with the FEM model and with Eq. (4) for different inclination angles β, under a damaged state, where the crack surface extends horizontally up to the center of the reinforcements cross-section.*

Inclined reinforcements:
Using now the same reinforcements, this time with an inclination of $\beta = 45°$, the new utilization factor will be computed. Accordingly, in a first step the forces $F_{r,V}$ and $F_{r,M}$ are obtained, where the limits used in equations (5) and (6) are given as (all values in mm)

$$y_{0,I} = 94 \; ; y_{1,I} = -47 \; ; y_{2,I} = -225 \qquad (14)$$

$$y_{0,II} = -94 \; ; y_{1,II} = 47 \; ; y_{2,II} = 225 \qquad (15)$$

for the section I and II are respectively.
With these limits applied to equations (5) and (6) the following values for the forces $F_{r,V}$ and $F_{r,M}$ are obtained:

$$F_{r,V,I} = 51.87kN \; ; \; F_{r,V,II} = 51.7 \; kN \qquad (16)$$

$$F_{r,M,I} = 289.1 \; kN \; ; \; F_{r,M,II} = -343.3 \; kN \; . \qquad (17)$$

These results are used in equation (4) to obtain the maximum axial force in the internal reinforcement:

$$F_{r,I} = 24.4 \; kN \; ; \; F_{r,II} = 23.3 \; kN \; . \qquad (18)$$

The utilization factor of the screws are then calculated, obtaining

$$\frac{F_{r,I}}{R_{ax}} = \frac{24.4}{32.0} = 0.76 < 1 \; . \qquad (19)$$

Although the utilization factors obtained for both examples (vertical and inclined screws) are very similar, it is important to notice, that this may not always be the case, for example with increasing rod diameters. In this case, the axial forces of the inclined reinforcements will increase, as compared to the current design method. This is mainly explained by the fact that in equation (4) is used implicitly the diameter of the reinforcement.
Also important to mention, is the fact that, regardless of the similar utilization factor obtained, the inclined reinforcement has the added effect of significantly reducing the shear stresses and the stresses perpendicular to grain in the periphery of the hole.

6 CONCLUSIONS

Using a parametric finite element model it was shown that internal reinforcements of beams with round holes, by means of glued-in steel rods or screws, placed perpendicular to beam axis, as described in the current version the German National Annex to EC5 [2], have a rather small impact on the stresses perpendicular to the grain at the periphery of the hole. Furthermore, the effect of the vertical reinforcements on the shear stresses is negligible. In order to overcome these deficiencies, the effect of inclined internal rod reinforcements was investigated numerically. These inclined reinforcements resulted in, depending on the rod inclination, a considerably more expressed reduction of peak stresses at the periphery of the hole. In the case of an angle of 45°, reductions between 30% and 40% were observed for both vertical tensile stresses and shear stresses, as compared to the unreinforced case.
A first draft of a design procedure is presented, based on the results of the FEM simulations introduced. At the present, the validity of this proposed equation is limited to the investigated configurations (100 mm < beam width < 120 mm and 12 mm < rod diameter < 18 mm). Real-size experiments will be further pursued in order to assess the effectiveness of inclined rods as reinforcements in beams with holes, and to validate the observations made with the FEM model presented here.

REFERENCES

[1] DIN EN 1995-1-1:2010, *Eurocode 5: Design of timber structures -- Part 1-1: General -- Common rules and rules for buildings; German version EN 1995-1-1:2004 + AC:2006 + A1:2008*, 2010.

[2] DIN EN 1995-1-1/NA:2013, *Nationaler Anhang -- National festgelegte Parameter -- Eurocode 5: Bemessung und Konstruktion von Holzbauten -- Teil 1-1: Allgemeines -- Allgemeine Regeln und Regeln für den Hochbau*, DIN-Deutsches Institut für Normung e.V., 2013.

[3] S. Aicher und L. Höfflin, „Glulam beams with holes reinforced by steel bars," in *CIB W 18, Proceedings Meeting 42*, Dübendorf, 2009.

[4] H. J. Blaß und I. Bejtka, Querzugverstärkungen in gefährdeten Bereichen mit selbstbohrenden Holzschrauben, Versuchsanst. für Stahl, Holz und Steine, Abt. Ingenieurholzbau, Universität Fridericiana Karlsruhe, 2003.

[5] S. Aicher, „Glulam Beams with Internally and Externally Reinforced Holes - Test, Detailing and Design," in *International Council For Research And Innovation In Building And Construction, Working Commission W18 - Timber Structures, Alghero, Italy*, 2011.

[6] EN 14080:2013, *Timber structures -- Glued laminated timber and glued solid timber -- Requirements*, 2013.

[7] C. Tapia und S. Aicher, „Rechnerische Untersuchungen zu Mindestabständen von Durchbrüchen in Brettschichtholz," in *Doktorandenkolloquium "Holzbau Forschung und Praxis'"*, Pfaffenwaldring 7, 70569 Stuttgart, 2016.